Contents

Contributors

Hans-Peter Gail Institut für Theoretische Astrophysik, Universität Heidelberg, Tiergartenstr. 15, D-69121 Heidelberg, Germany.
e-mail: gail@ita.uni-heidelberg.de

Erwin Sedlmayr Institut für Astronomie und Astrophysik, Technische Universität Berlin, Hardenbergstr. 36, D-10623 Berlin, Germany.
e-mail: sedlmayr@physik.tu-berlin.de

1
Dust formation in M stars

Hans-Peter Gail
Institut für Theoretische Astrophysik, Universität Heidelberg

and

Erwin Sedlmayr
Institut für Astronomie & Astrophysik, Technische Universität Berlin

1 Introduction

Stars with initial masses between $\approx 2\,M_\odot$ and $\approx 8\,M_\odot$ on the main sequence develop first through the Red Giant phase until they ignite central helium burning. Later they start to climb up the Asymptotic Giant Branch (AGB) where they alternately burn helium and hydrogen in two thin shells over a degenerated carbon-oxygen core. In this stage, the thermal pulsing ABG stage (TP-AGB), they are cool ($T_{\rm eff} \approx 2000 - 2500\,$K), luminous ($L \approx 10^4\,L_\odot$) and very extended ($R_* \approx 10^3\,R_\odot$) giant stars. For further discussion see Chapter 11. Observationally they are found to be emitters of a strong infrared emission and a rich zoo of molecular microwave emission lines which originate in a dense and very extended ($\gtrsim 10^4\,R_*$) circumstellar shell of cool gas and dust. The central stars are usually obscured by the circumstellar dust and in many cases they are even optically invisible and can only be identified by the IR-emission from warm dust and by microwave molecular line emission.

The most intense molecular lines are usually the thermally excited emission lines of CO and in many cases very strong maser emission lines of OH, H_2O and SiO are observed (see, e.g., the excellent review of Habing 1996). A common characteristic of all the lines is the large velocity extent of more than $20\,{\rm km\,s^{-1}}$ which is simply interpreted as being the result of an expanding circumstellar envelope. Quantitative analysis of the line emission yields mass-loss rates ranging from less than $10^{-7}\,M_\odot\,{\rm yr^{-1}}$ for optically visible objects with only a slight far-IR excess emission by the circumstellar dust up to more than $10^{-4}\,M_\odot\,{\rm yr^{-1}}$ for the most heavily obscured OH-IR-objects. The expansion velocity is usually found to be in the range between 10 and $25\,{\rm km\,s^{-1}}$ (cf. Loup et al. 1993).

According to observations there exist two different classes of objects with circumstellar dust shells with distinctively different chemical composition: (i) stars of spectral type M (if the stellar atmosphere is visible) for which abundant oxygen bearing molecules and only trace amounts of carbon bearing molecules (besides the abundant CO molecule) are observed to exist in their atmospheres and their circumstellar shells, and (ii) stars of spectral type C which show a rich zoo of abundant carbon bearing molecules and only trace amounts of oxygen bearing molecules[1]. M stars mainly form silicate dust in their circumstellar shells, as can be seen by strong infrared features at $10\,\mu$m and $18\,\mu$m usually ascribed to stretching and bending vibrational modes in a SiO_4 group, while C stars form carbon dust, as is inferred from the strong featureless continuous absorption of the main circumstellar dust component in such objects (see Dorschner and Henning 1995, and references therein). Minor dust components are likely to be formed besides the main components in both cases (e.g. Dorschner and Henning 1995, Waters et al. 1996,) and exceptions to the above general relation between spectral type of the central star and nature of the main condensate are known (e.g. Sylvester et al. 1994).

These differences in the chemical composition of the mixture of molecules and dust are related to the relative element abundances of oxygen and carbon. In stars of spectral type M the oxygen abundance exceeds that of carbon ($\epsilon_{\rm O} > \epsilon_{\rm C}$) while in stars of spectral class C carbon is the more abundant ($\epsilon_{\rm C} > \epsilon_{\rm O}$) of the two elements. These differences in abundance result from a convective mixing between the central regions of the star subject to shell burning and the stellar surface in some fraction of the TP-AGB stars (e.g. Iben 1991). In this "third dredge up", operating at the top of the AGB, ashes of the He to C burning process are brought to the surface. The mixing then gradually increases the C abundance relative to the O abundance. As is well known the exceptionally high bond energy between C and O in the CO-molecule results in a chemical blocking of the less abundant of the two elements C and O in the unreactive CO molecule. This blocking of C in M stars and of O in C stars is responsible for the observed different chemical compositions of the gas phase and for the formation of silicate dust and probably some other oxide dust components in circumstellar shells of M stars and of soot, SiC and probably some additional non-oxide dust components in the case of C stars (e.g. Gail and Sedlmayr 1987).

The nature of the dust material formed and the possible chemical pathways for the nucleation and growth of circumstellar dust obviously depends crucially on the element mixture in the stellar outflow. This element mixture is fixed by the initial composition of the star at the time of its formation and by the nuclear burning processes operating deep within the star which results by means of convective mixing processes in certain compositional changes at the stellar surface in late stages of the stars evolution.

Intermediate mass stars in the range $2M_\odot \lesssim M \lesssim 8M_\odot$ have stellar lifetimes small compared to the age of our Galaxy. They are formed therefore from material with a mixture of elements not much different from that observed for early type main sequence stars or that derived for the Solar System. This standard cosmic element mixture (Anders and Grevesse 1989, Grevesse and Noels 1993) is

[1] We ignore here the rare transition objects of spectral class S between spectral classes M and C.

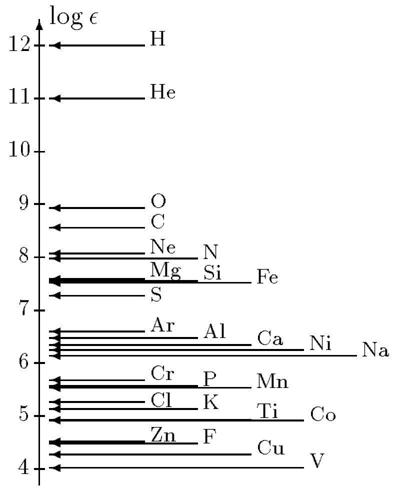

FIG. 1. Solar relative abundances of the most abundant elements according to Anders and Grevesse (1989) and Grevesse and Noels (1993).

shown in Fig. 1 for the most abundant elements. The only elements shown in this figure are those likely to be involved in the dust formation process, and only the most abundant ones can be involved in the formation of the dust component(s) responsible for the strong extinction of the circumstellar dust shell.

The remaining elements have cosmic abundances that are much too low to form visible dust or to form significant numbers of seed nuclei for the growth of dust from the more abundant elements. Exceptions are possible only if very strong abundance excesses of such rare elements occur. The element abundances of M-giants have been studied, e.g., by Smith and Lambert (1990).

Despite its obvious astrophysical relevance no adequate descriptions of inorganic cluster and grain formation are available. The reason for this shortcoming lies in the enormous complexity of the various microphysical processes involved, in the lack of most of the required data necessary for a reliable modelling of the cluster structures, and in the heterogeneous nature of the condensates. Therefore, the approaches applied so far are forced to adopt strongly simplified descriptions like liquid droplet models, chemical homogeneity, and well defined mineralogical structures (e.g. Kozasa and Hasegawa 1987), yielding valuable insight into basic features of the dust formation process and into the complexity of the whole problem but of course cannot provide reliable quantitative predictions.

By a broad discussion of the astrophysical situation, the applied theoretical description and some key condensates expected in this context, this Chapter tries to shed light on important problems aiming to establish a more secure foundation on which more realistic future developments can be based.

2 Dust nucleation

The starting point of the classical theory of formation of seed particles for dust growth is to consider the formation of a cluster by the stepwise collection of a single molecular species A_1 (the monomer) from the gas phase

$$A_1 \xrightarrow{A_1} A_2 \xrightarrow{A_1} A_3 \xrightarrow{A_1} A_4 \xrightarrow{A_1} A_5 \xrightarrow{A_1} \cdots$$

More complicated processes involving cluster growth by addition of several different molecular species from the gas phase and by chemical surface reactions are not considered in homogeneous nucleation theory.

2.1 Equilibrium condensation

In the following we characterise each cluster by the number N of the basic molecules required for its formation and denote its particle density by $f(N,t)$ and its partial pressure in the gas phase by $p(N)$. The distribution of the partial pressures of clusters with size N in a thermodynamic equilibrium state is given by the law of mass action

$$\overset{o}{p}(N) = p^N(1)\, \exp[-\Delta G(N)/RT] \tag{2.1}$$

where ΔG is the free enthalpy of formation of the cluster of size N from N monomers. This generally is rewritten in terms of the vapour pressure $p_{\rm vap}$ of the monomers over the condensate to obtain

$$\overset{o}{p}(N) = \exp[N \ln S' - \Delta(G(N) - NG(\infty))/RT] \tag{2.2}$$

where $\Delta G(\infty)$ is the free enthalpy of formation of the monomer from the condensate and S' is the supersaturation ratio

$$S' = p/p_{\rm vap}\,. \tag{2.3}$$

p is the actual partial pressure of the monomers $N = 1$ in the gas phase; this is identical with $\overset{o}{p}(1)$. The monomer pressure is determined by the requirement

$$\sum_{N=1}^{\infty} N \overset{o}{p}(N) = f_\epsilon \epsilon P_{\rm H}\,. \tag{2.4}$$

$P_{\rm H}$ is the fictitious pressure of hydrogen nuclei if they all were present as free particles, ϵ is the element abundance of the least abundant element required to form the monomer and $1 - f_\epsilon$ is the fraction of this element which is contained in other molecular species which do not participate in the condensation process[2].

[2] In the case of carbon dust formation, for instance, $1 - f_\epsilon$ equals the fraction of the carbon bound into CO, because the C bound into CO cannot be condensed into dust. For condensation of dust in M stars such a blocking of some fraction of a condensible element in some strongly bound and unreactive molecular species seems not to occur, such that we have always $f_\epsilon = 1$ in this case.

Another way of writing (2.1) is

$$\overset{o}{p}(N) = p^N(1)\,\frac{U_N(T)}{U_1^N(T)}\,\mathrm{e}^{-\Delta E_N/kT}\,(kT)^{-(N-1)} \tag{2.5}$$

where $U_N(T)$ and $U_1(T)$ are the partition functions of a cluster of size N and the monomer, respectively, and ΔE_N is the energy of formation of the N-cluster from N monomers. The partition functions U are determined by the translational and internal energy states of the particle. A calculation of $\overset{o}{p}(N)$ from (2.5) requires besides the bond energy a complete knowledge of the vibrational and rotational energy spectrum of the clusters and in some cases also of the spectrum of their excited electronic states.

The difference of the free enthalpies

$$\Delta(G(N) - NG(\infty)) = \Delta H_f(N) - N \cdot \Delta H_f(\mathrm{cond.}) + T\Delta S \tag{2.6}$$

is essentially determined by the difference of the bond energy of the monomers in the finite cluster of size N and of that in the infinitely extended condensate. This energy difference is positive since the bond energy of monomers in the solid is higher than in a finite cluster. To some extent the difference of the Gibbs enthalpy depends also on the difference between the partition functions for the translational and internal degrees of freedom, which determines ΔS, but this contribution usually is neglected in *classical* nucleation theory.

To determine the energy defect $\Delta H_f(N) - N\Delta H_f(\mathrm{cond.})$ *classical* nucleation theory assumes that this can be calculated from the macroscopic surface energy of the bulk condensate which is given in terms of the surface tension σ and the surface area A_N of the particle by

$$\Delta H_f(N) - N \cdot \Delta H_f(\mathrm{cond.}) \;= \sigma A_N\,. \tag{2.7}$$

This basic assumption of *classical* nucleation theory is the source of the observed discrepancies (see Donn and Nuth 1985) between its predictions and experimental results. It takes for granted that the bond properties at the molecular level are essentially the same as for the infinitely extended condensate, but this is not true in real cases. Nevertheless, it is worthwhile to consider this simple approach further since the fundamental concepts of any nucleation theory can be demonstrated most easily for this model.

A second assumption usually introduced in classical nucleation theory is that the small clusters have spherical size. This allows a calculation of the surface area of the cluster in a simple way and one obtains the following expression for the dependence of ΔG on cluster size N

$$\Delta G = -RTN\ln S' + 4\pi\sigma\left(\frac{3V_0}{4\pi}\right)^{\frac{2}{3}} N^{\frac{2}{3}} - T\Delta S \tag{2.8}$$

where V_0 is the volume occupied by one monomer in the condensed phase. The essential conclusions which can be drawn from this are:

(1) If the supersaturation ratio S' is less than unity then ΔG increases monotonically with increasing cluster size N. The size distribution of clusters according to (2.2) monotonically decreases with increasing N. Observable quantities of clusters exist only on the molecular level. No macroscopic sized dust grains exist.

(2) If the supersaturation ratio S' exceeds unity then ΔG depends in a more complicated way on N. The first term in (2.8) *decreases* linearly with increasing N while the second one *increases* somewhat more slowly with N, proportional to $N^{\frac{2}{3}}$. For sufficiently big N the first term dominates and ΔG decreases with increasing cluster size. The size distribution then *increases* with increasing N as

$$\overset{o}{p}(N) \propto S'^N \,. \tag{2.9}$$

In this case according to the constraint (2.4) most of the mass would be contained in a few very big clusters. The case $S' > 1$, thus, corresponds to complete condensation in thermodynamic equilibrium.

(3) For small N usually the second term dominates in (2.8). The size distribution then *decreases* with increasing N for small cluster sizes. Since for large N it has to satisfy (2.9) there necessarily exists some cluster size N_* where $\overset{o}{p}(N)$ has an absolute minimum. For very large supersaturation ratios, S', the first term in (2.8) dominates for all cluster sizes N. Then (2.9) holds for all $N \geq 1$ and the critical cluster size N_* where $\overset{o}{p}$ takes a minimum in this case is simply $N_* = 1$. The existence of this critical cluster size N_* where $\overset{o}{p}$ takes its absolute minimum is crucial for the whole nucleation problem, as we shall see below.

Realistic calculations of cluster abundances have to be based on detailed theoretical and experimental determinations of thermochemical functions for clusters up to sufficiently large size N (> 10 at least) for the species which may be involved in the nucleation process. Examples for such calculations are presented in Sect. 3.

2.2 Classical homogeneous nucleation theory

Nearly all attempts to calculate the formation of condensation nuclei in the outflows of cool stars up to now have been based on the approach of classical homogeneous nucleation theory, starting with Donn et al. (1968). The essential principles of applying this approach to dust condensation in circumstellar shells are outlined in (among many others): Salpeter (1974), Draine and Salpeter (1977), Yamamoto and Hasegawa (1977), Draine (1979), Deguchi (1980), Gail et al. (1984), Gail and Sedlmayr (1986), Sedlmayr and Dominik (1995).

Basically the formation of clusters can be conceived as the product of a chain of chemical reactions resulting in a production rate of critical clusters (e.g. Gail and Sedlmayr 1988, Köhler et al. 1997)

$$J_* = \left[\sum_{i=1}^{N_{\rm max}} \frac{\tau_{{\rm gr},i}}{\overset{o}{f}(i)} \right]^{-1} , \tag{2.10}$$

which in case of a strong supersaturation, where $\overset{o}{f}(N)$ has a sharp minimum at $N = N_*$, can be approximated by the term

$$J_* = \frac{\overset{o}{f}(N_*)}{\tau_{{\rm gr},N_*}} . \tag{2.11}$$

Thus we have the very plausible result that *the rate of dust particle formation is determined by the slowest growth step on the reaction chain along clusters of increasing size which occurs at the cluster size N_* where $\overset{o}{f}(N)$ is smallest.*

A calculation of the nucleation rate in circumstellar dust shells requires, then, the knowledge of the species which may be responsible for nucleation and the properties of all clusters formed from the relevant species. For a given thermodynamic state of the gas phase it is possible then to calculate the equilibrium abundances of all clusters and from this to determine the critical cluster size N_* and the nucleation rate J_*.

In the approximation of homogeneous classical nucleation theory, the equilibrium pressure $\overset{o}{p}$ of the clusters is given by (2.2) with ΔG given by (2.8). For evaluating the sum over N it is approximated by an integral which then is calculated by means of the saddle-point integration method. The result is (e.g. Feder et al. 1966)

$$J_* = \sqrt{\frac{2\sigma}{\pi m}}\, V_0\, n_1^2\ \exp\left[-\frac{16\pi\sigma^3 V_0^2}{3k^3T^3(\ln S')^2} \right] . \tag{2.12}$$

m is the mass and n_1 the particle density of the monomer, V_0 the volume occupied by the nominal monomer in the bulk condensate and σ is the surface tension. This equation allows a calculation of the nucleation rate from the properties of the condensate, its surface tension, and its vapour pressure. Up to now in astrophysics, considerations of condensation have been nearly exclusively based on this expression for J_*. The main objections against this approach, and its main shortcomings, are listed by Donn and Nuth (1985). Nevertheless (2.12) is generally used since no realistic theory of condensation in an oxygen rich environment is known at present.

An interesting application of (2.12) has been made by Nuth and Donn (1982b) to the condensation of SiO. The SiO molecule is one of the few molecules with exceptionally high bond energy (cf. Fig. 3) and is stable even in the atmospheres of cool stars. It forms a pure SiO solid with a condensation temperature of approximately 1 000 K in the laboratory. For this reason it has often been thought to be responsible for the initiation of dust condensation in circumstellar shells (e.g. Nuth and Donn 1982b, Gail and Sedlmayr 1986). Nuth and Donn (1982b) measured the nucleation rate J_* for SiO in the laboratory by evaporating and re-condensing SiO and fitted their results for J_* with the expression (2.12). The parameters $m = 7.3\,10^{-23}\,\mathrm{g}$, $V_0 = 2.4\,10^{-23}\,\mathrm{cm}^3$ are fixed by the properties of the condensate. The vapour pressure of SiO molecules over solid SiO is

$$p_{\mathrm{vap}} = 760\exp\left[12.81\left(1 - \frac{2300.9}{T}\right)\right] \tag{2.13}$$

(in Torr). By fitting the experimental data with (2.12) Nuth and Donn (1982b) determined a fictitious surface tension $\sigma = 500\,\mathrm{dyn\,cm}^{-2}$. This σ in principle has nothing to do with a real surface tension but merely is that value of the parameter σ which yields the best approximation of the experimentally determined values of J_* by a relation of the type (2.12). Thus, a calculation of J_* for SiO nucleation from (2.12) with this value of σ yield results which are not subject to the usual errors of classical nucleation theory.

Figure 2 shows lines of constant nucleation rate in the P-T plane calculated by this approach for an element mixture of standard composition. An inspection of the figure shows that dust formation by nucleation of SiO does not occur until the temperature of the outflowing gas has fallen below 500 K. This is incompatible with a dust temperature of $\approx 1\,000$ K in the dust condensation zone derived from models for the circumstellar IR-emission of optically thick dust shells. Therefore, SiO nucleation cannot be responsible for the condensation in these objects. There remains the possibility, however, that SiO triggers dust formation in *optically thin* dust shells where condensation temperatures as low as this are observed in many cases (Rowan-Robinson and Harris 1983).

2.3 Possible nucleation species

We are now able to state some rules which a particular species from the gas phase has to satisfy in order to be a favourable candidate for nucleation:

(1) The nucleation rate depends on the product of the number density of the monomer (via the collision rate) and the number density of the critical cluster. Thus, the least abundant element in the molecule should have an element abundance as high as possible in order that this product may become as large as possible.

(2) For nucleation to occur at a temperature as high as possible the monomer should already be formed at a temperature as high as possible. This requires an exceptionally high bond energy.

(3) Unlimited growth beyond some critical cluster size requires that the thermodynamic equilibrium size distribution $\overset{o}{p}(N)$ beyond the critical cluster size N_* increases indefinitely with increasing cluster size N. This is possible only if the gas phase is supersaturated with respect to the formation of the solid condensate from the monomer and this in turn requires that the solid condensate formed from the monomer vaporises at a temperature as high as possible.

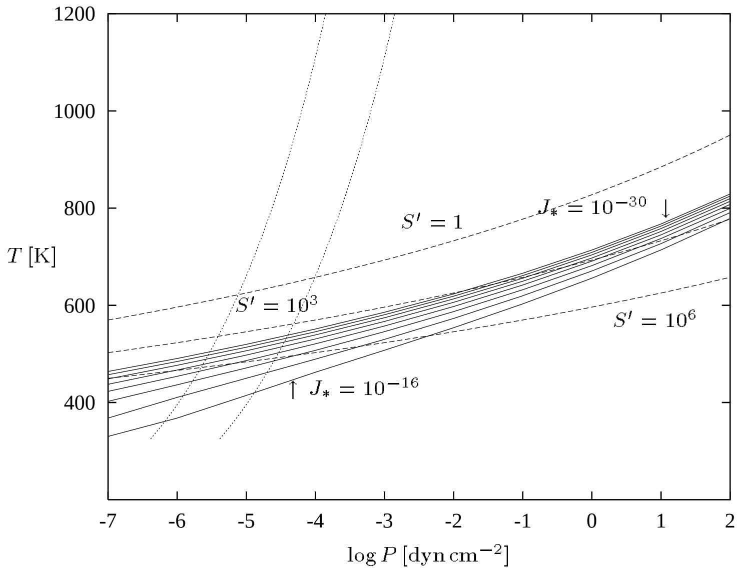

FIG. 2. Supersaturation ratio S' (dashed lines) and nucleation rate J_* (full lines) for SiO. J_* (seed nuclei per sec and H-nucleus) is shown from $J_* = 10^{-30}$ (top) to $J_* = 10^{-16}$ (bottom) in steps of $\Delta \log_{10} J_* = 2$. The dotted lines show the P-T combinations of a stationary stellar wind at the sonic point for $\dot{M} = 10^{-6}\, M_\odot\, \mathrm{yr}^{-1}$ (left) and $10^{-5}\, M_\odot\, \mathrm{yr}^{-1}$ (right).

(4) The nucleation rate depends on the probability that two particles stick together on collision. This probability should be as high as possible. This requires reactive molecules, radicals if possible, and an efficient way of removing the reaction energy, or alternatively the possibility of transferring (part of) this energy to internal degrees of freedom which later are de-excited, for instance by radiative transitions.

Figure 3 shows the bond energy of diatomic molecules with bond energies exceeding 4 eV for the more abundant elements. An inspection of this figure shows that there are only a few abundant molecular species with exceptional high bond energies which are possible candidates for forming the first clusters in the outflow of M stars. These are listed in Table 1. Additionally, the two abundant elements Mg and Fe from which refractory condensates may be formed are present in the gas phase as free atoms. Other abundant species like H_2, CO, H_2O, and N_2 need not be considered since they condense at a very low temperature (some may condense as ices in the outermost parts of dense circumstellar shells).

At first glance, the SiO molecule seems to be the most likely candidate for nucleation since it satisfies both of the conditions: a bond energy as high as possible, and a high abundance. It violates, however, the third requirement and, indeed, in Sect. 2.2 we showed that SiO is not a likely candidate for nucleation.

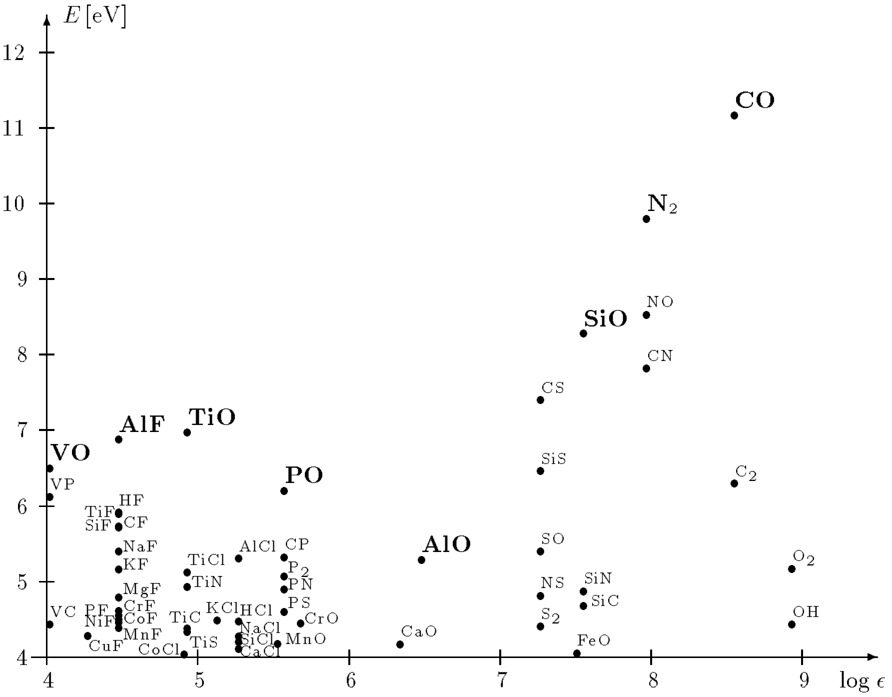

FIG. 3. Bond energies of particular strongly bound diatomic molecules of abundant elements, plotted against the abundance of the less abundant of its constituents. (Bond energies from Lide 1995).

The next most abundant species in the gas phase which might be responsible for initiation of dust condensation are Fe and Mg. They are shown in Sect. 3.2 not to be responsible for circumstellar nucleation.

For other species from Table 1 no definite conclusion can be drawn at present with respect to the likelihood of their responsibility for nucleation. From the point of view of element abundance, aluminium- or titanium oxide clusters seem to be favoured. Due to the low abundance of F and Zr AlF and ZrO can be important only if nucleation of the former two species does not work.

3 Examples for the calculation of nucleation rates

Realistic calculations of cluster abundances have to be based on detailed theoretical and experimental determinations of thermochemical functions for clusters up to sufficiently large size N (> 10 at least) for all of the species which may be involved in the nucleation process. Such calculations are just beginning to become available. We present here two examples, the formation of MgO and Fe clusters.

Table 1 Molecules with exceptional high bond energy D and their electronegativity difference Δ.

Molecule	SiO	AlO	TiO	AlF	ZrO
D [eV]	8.28	5.29	6.97	6.88	8.04
Δ	1.7	2.0	2.0	2.5	2.1

3.1 MgO clusters

The properties and thermodynamic functions for MgO clusters up to a cluster size of $N = 16$ have been studied by Köhler, Gail, and Sedlmayr (1997). This species was thought to be important for condensation in circumstellar shells at the time that work was begun, but since then the dissociation energy of MgO has considerably been revised downwards and now MgO is unlikely to be important for the circumstellar dust problem. The calculation of a nucleation rate is, however, a pretty example which demonstrates along which lines one has to proceed in the future to solve the problem of circumstellar dust nucleation.

The magnesium oxide solid is believed to be a pure ionic compound formed from Mg^{++} cations and O^{--} anions, respectively. The crystal structure of the solid is of the NaCl lattice type. The properties of such ionic crystals can well be described by the classical Born-Mayer potential model, as is well known from solid state physics. The total potential energy is assumed to be given by

$$\Phi = -\tfrac{1}{2}\sum_{\substack{i,j\\ i\neq j}} \frac{Z_i Z_j e^2}{r_{ij}} + \tfrac{1}{2}\sum_{\substack{i,j\\ i\neq j}} A\mathrm{e}^{-\frac{r_{ij}}{\rho}} \,. \tag{3.1}$$

r_{ij} is the mutual distance between the ions i and j, Z_i and Z_j are their charges (± 2 for MgO), ρ_{ij} measures the steepness and A_{ij} the strength of the repulsive potential between the ions due to overlap of their outer electron shells. The summation is over all ions in the crystal. Usually, A_{ij} and ρ_{ij} are assumed to be independent of i and j. This model works quite well for the solid (e.g. Evans 1966) and allows a calculation all of its properties, if the two parameters A and ρ are determined by a fit to two measured quantities. For the alkali halides this approach also works quite well for the free molecule with a single set of parameters A and ρ describing both the properties of the molecules and the solid. The potential model (3.1) has been used with great success, for example, in calculating the cluster properties for NaCl clusters (Martin 1983).

The same potential model may be applied to other compounds with strong ionic character of the chemical bond, for instance the alkaline earths. Though their electronegativity difference is not as big as that of alkali halides, the solids form ionic crystals which are well described by Born-Mayer theory (e.g. Evans 1966). Application of the potential model (3.1) to the free molecule, however, yields unsatisfactory results. The main reasons for this shortcoming are:

- The ions are polarised in the local electric field due to the other ions. In the NaCl-type lattice of the solid there is no net polarisation for symmetry

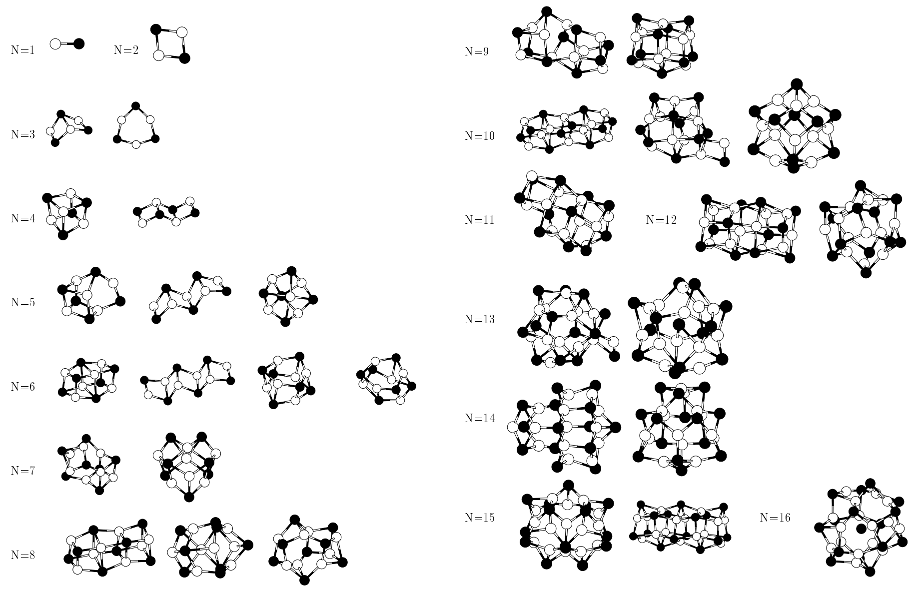

FIG. 4. Structures of MgO clusters for clusters of size $N = 1, \ldots, N = 16$ and their isomers. The ground state configuration is the leftmost one, the bond energy of isomers decreases from left to the right (for more details see Köhler et al. 1997).

reasons, but for small clusters without such high a symmetry the induced-dipole – monopol interaction contributes to the total energy.

- The bond in alkaline earth compounds has a considerable covalent contribution. The attraction cannot be described by coulomb-forces alone.
- Due to the lower electronegativity difference the ions carry only fractional charges.
- In the free alkaline earth molecule the ions are only singly charged and not double charged as in the solid.

In Köhler et al. (1997) the potential model (3.1) was modified by including the polarisation of the ions, an additional Morse-potential like contribution to the particle-particle interaction potential and allowing for a size dependent fractional charging of the ions

$$\Phi(N) = \sum_{\substack{i,j \\ i>j}} \left[A\,\mathrm{e}^{-\frac{2r_{ij}}{\rho}} - B(N)\,\mathrm{e}^{-\frac{r_{ij}}{\rho}} - \frac{Z_{\mathrm{eff},i} Z_{\mathrm{eff},j}\, e^2}{r_{ij}} \right] - \frac{1}{2} \sum_{\substack{i,j \\ i>j}} \frac{Z_{\mathrm{eff},i}\, e\, \vec{\mu}_j \cdot \vec{r}_{ij}}{r_{ij}^3} \tag{3.2}$$

$B(N)$ is an additional covalent attractive contribution to the potential, depend-

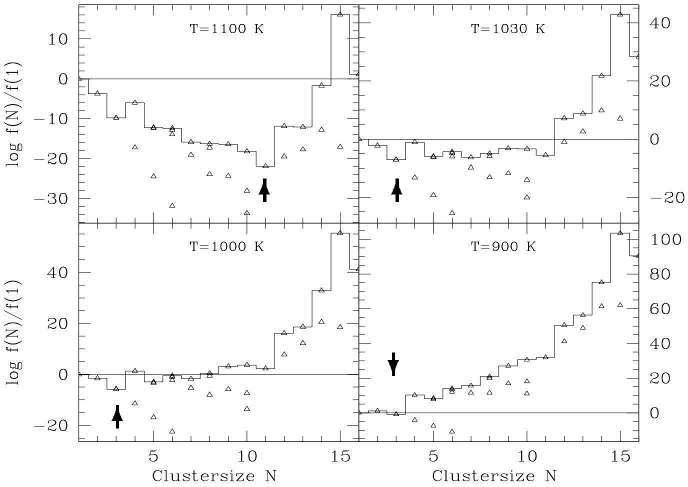

FIG. 5. Density of MgO clusters relative to the monomer density for four different temperatures and a typical gas density of $n_{H_2} = 10^{10}\,\mathrm{cm}^{-3}$. The full line connects the most abundant clusters of each size, triangles below of this correspond to less tightly bound isomers. If the full curve decreases for small cluster sizes and increases for large cluster sizes, nucleation occurs. In this case, the least abundant cluster on the curve defines the critical cluster for nucleation (marked by a thick arrow).

ing on cluster size N, $Z_{\mathrm{eff},j}$ is the (size dependent) fractional charge, and

$$\vec{\mu}_j = \alpha_j \sum_{\substack{k \\ k\neq j}} \frac{Z_{\mathrm{eff},k}\, e\, \vec{r}_{kj}}{r_{kj}^3} \tag{3.3}$$

is the induced dipole moment on particle j where α_j denotes its polarizability.

This potential model has been used to calculate the structure and properties of MgO clusters. The parameters of the potential were determined by a fit to (i) the bond energy and (ii) the vibrational frequency of the molecule and (iii) to the crystal lattice energy. The ground state of a cluster of size N with N cations Mg^{++} and N anions O^{--} each was calculated by determining the minimum of the potential (3.2) in the $6N$-dimensional configuration space $(\vec{x}_1, ..., \vec{x}_{2N})^{\mathrm{T}}$ of all ion positions. Possible isomers where determined by searching for all deep local minima of Φ with an energy no more than a few eV above the ground state. The structure of the first 16 MgO clusters and their isomers are shown in Fig. 4.

Once the cluster structures are known it is a simple task to calculate the moments of inertia and the vibrational frequencies from the eigenvalues of the force matrix. With these data and the calculated bond energies one readily calculates the free enthalpy of formation $\Delta G(N,T)$ of a $(\mathrm{MgO})_N$-cluster from N MgO molecules. The partial pressures $\overset{o}{p}(N)$ of clusters in thermodynamic

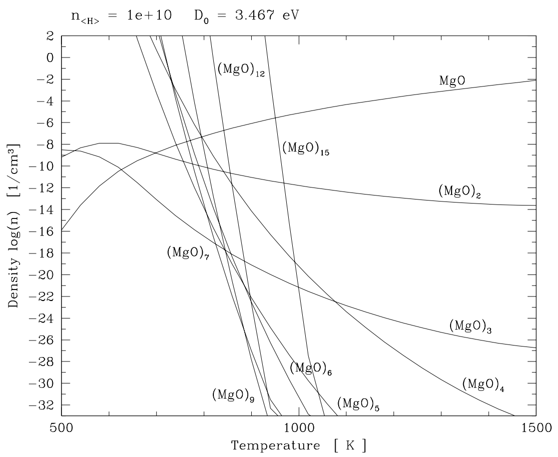

FIG. 6. Cluster densities for clusters of size $N = 1, \ldots, N = 15$ in chemical equilibrium with the monomer at a hydrogen density of $n_{\mathrm{H}_2} = 10^{10}\,\mathrm{cm}^{-3}$ which is typical for the condensation zone.

equilibrium are given by (2.5). Results for the cluster densities relative to the monomer density for a characteristic hydrogen density of $10^{10}\,\mathrm{cm}^{-3}$ in the dust condensation zone of a circumstellar shell are shown in Fig. 5. The full line corresponds to the ground states of the clusters. This line shows the expected behaviour for condensation to occur: a general decrease for small cluster sizes and a general increase for large cluster sizes. Considerable fluctuations around this general trend for individual clusters, however, are obvious. The cluster with least abundance along this line defines the critical cluster for nucleation which has to be used in eqn (2.10) for calculating the nucleation rate J_*. Fig. 6 shows the results for the true cluster density. In this representation, the lower envelope of the family of curves shown in Fig. 6 defines the density of the critical cluster.

For the case of MgO the resulting nucleation rate obviously is much too low for MgO to become important for dust nucleation. The calculation of Köhler et al. (1997) demonstrates, however, the way in which a nucleation rate has to be determined for real situations.

3.2 Iron clusters

Iron atoms are one of the most abundant species in the gas phase which may be involved in circumstellar dust formation process, and the iron metal is one of the most stable condensates which may be formed (cf. Fig. 9). For this reason the clustering of iron atoms is a possible candidate for the process initiating dust formation. Following the above general concepts outlined for MgO, John (1995) has calculated the nucleation rate by clustering of Fe atoms. Obviously, the particle-particle interaction cannot be described by a potential model of the Born-Mayer type in this case. The bond energy of the iron clusters, instead, is available from the laboratory experiments of Lian et al. (1992) for cluster

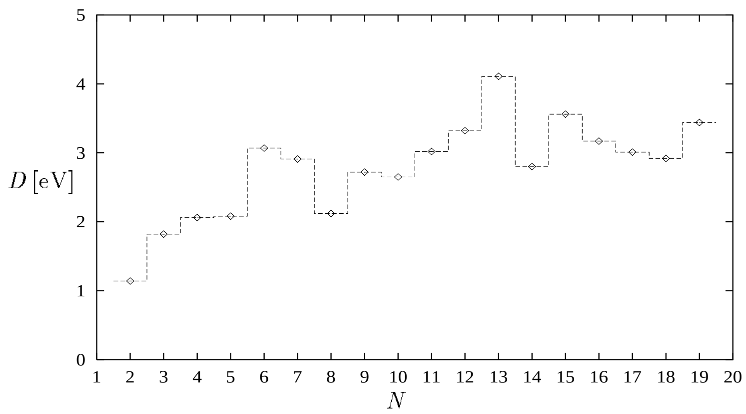

FIG. 7. Dissociation energy D (eV) of a single iron atom from an iron cluster of size N.

sizes up to $N = 19$. These are shown in Fig. 7. It is important to note that there is a very strong dependence of the bond energy of an iron atom within a cluster on the cluster size. The bond energy for small cluster sizes, particular for $N = 2, 3$, is very small. The equilibrium abundance of clusters with such a low dissociation energy clearly is extremely low at the temperature of $\approx 1\,000\,\mathrm{K}$ in the dust formation zone. They are stable only at much lower temperature and since during nucleation of iron each particle has to pass trough the stage $N = 2, 3$, we expect iron nucleation to be efficient only for temperatures $T \ll 1\,000\,\mathrm{K}$.

In order to derive the nucleation rate of Fe, John (1995) determined all the quantities required to calculate $\Delta G(N, T)$. The vibrational frequencies for the dimer and trimer are known from laboratory measurements, and for bigger clusters they are estimated from semi-empirical rules based on Debye theory. John (1995) derived the possible equilibrium configurations of Fe atoms in the clusters up to a cluster size $N = 19$ and calculated from this the moments of inertia for the clusters. The contribution of low lying electronic states to the partition function is particularly important in case of iron clusters. For the dimer these are known from quantum mechanical calculations (Shim and Gingerich 1982), and for bigger clusters the contribution of such states is estimated from a semiempirical interpolation procedure between the dimer case and the free electron model of the bulk condensate. From these data the free enthalpy of formation of clusters of size N from N free atoms is calculated. Details of this calculation will be published elsewhere (John et al. 1998). Results for the cluster densities relative to the monomer density for a characteristic hydrogen density of $10^{10}\,\mathrm{cm}^{-3}$ in the dust condensation zone of a circumstellar shell are shown in Fig. 8. The dependence of the normalized partial pressures on N shows the expected behaviour for condensation to occur: a general decrease for small cluster sizes and a general increase for large cluster sizes. Considerable fluctuations around this general trend for individual clusters are again observed.

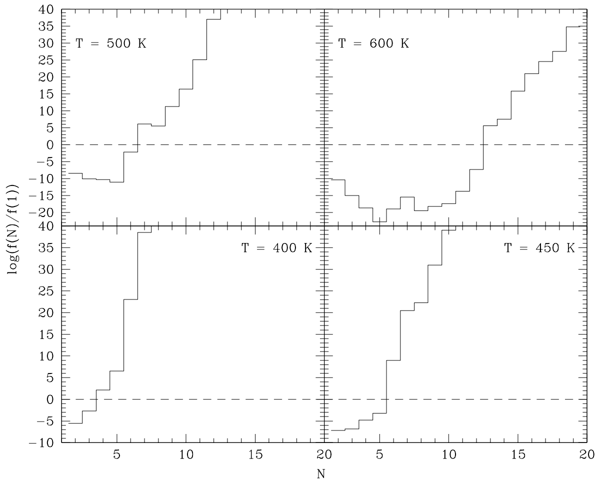

FIG. 8. Density of Fe clusters relative to the monomer density for four different temperatures and a typical iron atom density of $n_{\mathrm{Fe}} = 4\,10^5\,\mathrm{cm}^{-3}$ in the dust condensation zone. If the density of clusters decreases for small cluster sizes and increases for large cluster sizes, nucleation occurs. In this case, the least abundant cluster on the curve defines the critical cluster for nucleation.

An inspection of Fig. 8 shows that efficient nucleation of iron cannot be expected to occur until the temperature has dropped below 500 K since the density of the critical cluster is extremely low otherwise. The dust formation in a circumstellar shell, thus, cannot be triggered by the onset of iron nucleation because this requires a temperature much lower than the typical temperatures inferred from models for the IR-emission from circumstellar dust shells.

The abundant Mg atoms in circumstellar outflows also cannot be responsible for nucleation. The dimer has a bond energy of only 0.09 eV and the principal trend for the N-dependence of cluster bond energies should be similar to that for iron. Thus, the onset of nucleation of Mg also occurs at a very low temperature.

3.3 Future prospects

The two examples above demonstrate the way in which one has to proceed in the future in order to arrive at a definite conclusion with respect to the primary nucleating species in circumstellar shells and in order to calculate the nucleation rate for circumstellar dust: one has to determine the structure and bond energies, the moments of inertia and the vibrational frequencies of all possible clusters of a given substance, and this has to be done for all substances which may be important for the nucleation problem. This is probably not such a difficult task as it might seem at first glance: only a few species can be important, see Sect. 2.3. For two of them we now have definite results:

- The most likely candidate for nucleation from the point of view of particle abundance and stability, the nucleation of SiO, is ruled out in most cases because the temperature for the onset of nucleation is much too low, as was shown in Section 2.2.

- The next most abundant possible species, the Fe atoms are not responsible for dust nucleation (see Section 3.2).

According to our discussion in Sect. 2.3 the next likely candidates for nucleation are Al_mO_n clusters or TiO-clusters, which remain to be investigated. These compounds have a strong ionic character of their bonding according to their big electronegativity difference (cf. Table 1) and, therefore, their structure and energy can be calculated by modelling their bond properties by a semiempirical potential model as that applied by Köhler et al. (1997) for MgO. Such potential models have been successfully applied in geophysics to calculate the properties of minerals (e.g. Catti 1986). Calculations based on such semi-empirical potentials for aluminium- and titanium oxide clusters are currently underway at our institutes.

4 Iron-magnesium-silicate compounds

4.1 Nature of the condensate

For reasons of element abundance it is generally thought that the dominating dust component in circumstellar shells around M stars is some kind of magnesium-iron silicate (cf. Fig. 1 and Dorschner and Henning 1995). Such silicates occur with two different types of lattice structures and chemical compositions:

- The orthosilicates with the composition $Mg_{2x}Fe_{2(1-x)}SiO_4$. They form a continuous series of compounds with $0 \leq x \leq 1$. The two members at the endpoints of this series are fayalite ($x = 0$) and forsterite ($x = 1$). The intermediate case is known as olivine.
- The metasilicates with the composition $Mg_xFe_{1-x}SiO_3$. They form a continuous series of compounds with $0 \leq x \leq 1$. The two members at the endpoints of this series are gruenerite ($x = 0$) and enstatite ($x = 1$). The intermediate case is known as orthopyroxene.

We now consider some aspects of the formation of the dominating dust component, which we believe sheds some new light on the circumstellar dust formation process.

Let us consider the formation of forsterite (Mg_2SiO_4) from the gas phase in a thermodynamic equilibrium state. In view of the chemical composition of the gas phase in the dust formation zone of a circumstellar shell the corresponding chemical reaction is

$$2\mathrm{Mg} + \mathrm{SiO} + 3\mathrm{H_2O} \longrightarrow \mathrm{Mg_2SiO_{4,solid}} + 3\mathrm{H_2}\,.$$

In chemical equilibrium the partial pressures of the gaseous species involved in this reaction have to satisfy the law of mass action

$$p_{\mathrm{H_2}}^3 = p_{\mathrm{Mg}}^2\, p_{\mathrm{SiO}}\, p_{\mathrm{H_2O}}^3\, K_p(T) \tag{4.1}$$

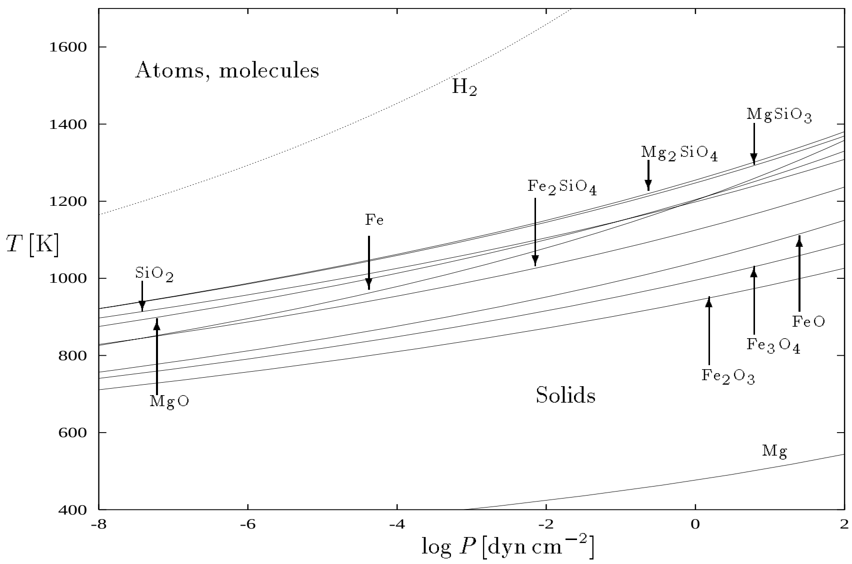

FIG. 9. Limit curves for destruction or growth of potential circumstellar condensates of the abundant refractory elements. Element abundances according to Anders and Grevesse (1989), thermodynamic data from Sharp and Huebner (1990). The dotted line is the limit curve for H_2 dissociation.

where

$$\begin{aligned} K_p(T) \;&=\; \exp\left[-\left(\Delta G(\mathrm{Mg_2SiO_4}) + 3\Delta G(\mathrm{H_2}) - 2\Delta G(\mathrm{Mg}) - \Delta G(\mathrm{SiO})\right.\right. \\ &\qquad\qquad \left.\left. -3\Delta G(\mathrm{H_2O})\right)/RT\right] \,. \end{aligned} \tag{4.2}$$

Let f be the fraction of the silicon bound in $\mathrm{Mg_2SiO_4}$. If there exists no other dust condensate, the partial pressure of H_2 in the gas phase is $\frac{1}{2}P_{\mathrm{H}}$, that of SiO is $(1-f)\epsilon_{\mathrm{Si}}P_{\mathrm{H}}$, that of Mg is $(\epsilon_{\mathrm{Mg}} - 2f\epsilon_{\mathrm{Si}})P_{\mathrm{H}}$, and that of water vapour is $(\epsilon_{\mathrm{O}} - \epsilon_{\mathrm{C}} - (1+3f)\epsilon_{\mathrm{Si}})P_{\mathrm{H}}$. Inserting this into (4.1) yields

$$P^3 = \frac{(1+2\epsilon_{\mathrm{He}})^3\, K_p^{-1}(T)}{2^6(1-f)\,\epsilon_{\mathrm{Si}}\,(\epsilon_{\mathrm{Mg}} - 2f\epsilon_{\mathrm{Si}})^2\,(\epsilon_{\mathrm{O}} - \epsilon_{\mathrm{C}} - (1+3f)\epsilon_{\mathrm{Si}})^3}\,. \tag{4.3}$$

For given f this defines a curve in the P-T plane on which the degree of condensation f of silicon into forsterite has just this value. The limit curve $f = 0$ for complete destruction of $\mathrm{Mg_2SiO_4}$ is shown in Figs. 9 and 10. If Mg is replaced by Fe in this equation, one obtains the corresponding equation for fayalite $\mathrm{Fe_2SiO_4}$. The limit curve $f = 0$ for complete destruction of $\mathrm{Fe_2SiO_4}$ is also shown in Fig. 9. We observe that forsterite is much more stable than fayalite. If the dust is formed in chemical equilibrium in a slowly cooling system, the magnesium silicate would be formed first. An inspection of Fig. 10 shows that circumstellar dust in equilibrium forms at a temperature of approximately 1 000 – 1 100 K, roughly consistent with the dust temperature derived for the dust formation

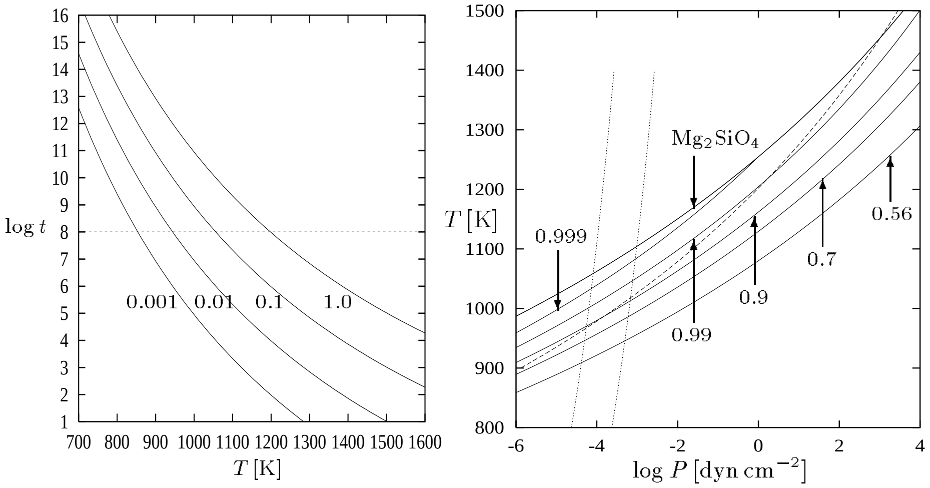

FIG. 10. Left part: Diffusion time scale (in s) for solid state diffusion in silicate dust particles of the indicated size (in μm). The horizontal dashed line indicates the characteristic timescale for temperature changes in the dust formation zone. Right part: Equilibrium composition of olivine. The numbers denote the value of the stoichiometric coefficient x for olivine with composition $Mg_{2x}Fe_{2(1-x)}SiO_4$. The uppermost full line is the stability limit of pure forsterite ($x = 1$). The dashed line shows the stability limit for condensed iron. The dotted lines shows the P-T stratification at the sonic point $v = c$ of a stationary stellar wind for $\dot{M} = 10^{-6}$ (left) and $10^{-5}\,M_\odot\,\mathrm{yr}^{-1}$ (right) for comparison.

zone of optically thick dust shells. Note that a formation of dust grains at this temperature requires growth on some pre-existing seed particles.

4.2 Annealing

At a sufficiently high temperature the dust is subject to the process of annealing. During this process the lattice vibrations in the dust become sufficiently excited that activation energy barriers can be overcome such that atoms or groups of atoms may change their position or their orientation within the lattice. The atoms in a poorly ordered or even amorphous dust material then start to rearrange and to migrate into energetically more favourable positions or orientations within the lattice, where they are more tightly bound and, then, become less mobile. By this process the dust material gradually develops some order in the local arrangement of the atoms and slowly changes its lattice structure to the locally ordered structure of a microcrystalline material. If amorphous dust grains contain a significant fraction of impurity elements within their lattice (for instance Al, Ca, and Na in a dust material of predominantly silicate composition) some kind of chemical fractionation may occur at the same time within the grain between the main component of the dust material and the impurities that were included during grain growth. These impurities may be driven out of the lattice and assemble at the surface or in separate inclusions. If annealing lasts sufficiently long complete crystallisation of the grains may even occur.

The essential microscopic processes responsible for annealing are diffusion of vacancies and interstitials, and self diffusion. For the purpose of an order of magnitude estimation these processes can be described by a rather simple model: if the particles perform a 3D random walk with constant step size a one has for the diffusion coefficient

$$D = \tfrac{1}{3} a^2 \nu \mathrm{e}^{-E_a/kT} \tag{4.4}$$

(e.g. Dekker 1963), where ν is the number of attempts per unit time for hopping to a neighbouring lattice site and E_a is the activation energy. The characteristic activation energy for silicate materials has been estimated by Lenzuni et al. (1995) and Duschl et al. (1996) to be $E_a = k \cdot 41\,000\,\mathrm{K}$ based on the annealing experiment of Nuth and Donn (1982a), and Nuth et al. (1986) for condensates from magnesium-silicate smokes and assuming the characteristic frequency ν to equal the average vibrational frequency of the SiO_4 tetrahedron. Essentially the same E_a results if one uses the Debye temperature $\Theta_D = 763\,\mathrm{K}$ for Mg_2SiO_4 (Kuskov and Galimzyanov 1986) for the determination of the characteristic frequency ν. We estimate the characteristic length a from the volume V of the basic molecule forming the lattice $V = Am/\rho = a^3$, where $A = 140.7$ is the molecular weight of Mg_2SiO_4, m the atomic mass unit and $\rho = 3.21\,\mathrm{g\,cm^{-3}}$ the mass density of Mg_2SiO_4. The coefficient of solid state diffusion within the silicate lattice is then

$$D = 1.2\,10^{-2}\ \mathrm{e}^{-41\,000\mathrm{K}/T}\ [\,\mathrm{cm^2\,s^{-1}}\,]\,. \tag{4.5}$$

In a 3D random walk the average rms displacement d^2 within time t is given by

$$d^2 = 3 \cdot 2Dt\,. \tag{4.6}$$

The left part of Fig. 10 shows the typical time t required for a single atom to walk over some prescribed distance d. This may be identified with the time required for annealing the amorphous structure of interstellar grains and to form a local crystal structure extending at least over regions of size d. Since the characteristic timescale for changes of the temperature in the outflow is of the order of 10^8 s and since the time scale for dust particle growth may be somewhat shorter, 10^7 s for instance, we infer from Fig. 10 that for a dust temperature of about 900 K initially amorphous circumstellar grains would start to develop some degree of local order in their lattice structure. At about 1 000 K the annealing of an amorphous silicate would take approximately one day (cf. Donn and Nuth 1982a) and at temperatures of about 1 100 K and above a long range order would develop within no more than $\approx 10^6$ s, consistent with the finding in a laboratory experiment with striated orthopyroxene which showed annealing of the structure by heating for one week to 1 100 K (Ashworth et al. 1984).

Recent observational findings (Goebel et al. 1994, Waters et al. 1996) indicate that the carriers of the circumstellar absorption bands show to some extent the structure which is compatible with at least a partial crystalline structure of the grain material and is less similar to that expected for an extremely amorphous structure, for instance like that proposed by Nuth and Hecht (1990). The grains are most likely hot enough in the dust formation zone ($T \gtrsim 900$ K) that solid state diffusion anneals part of the amorphous structure which probably first develops during surface growth from the gas phase (Gail and Sedlmayr 1984). The findings of the modelling of a large sample of circumstellar shells around M stars by Rowan-Robinson and Harris (1983) corroborates this, since they found for most of their objects with dense circumstellar shells condensation temperatures of $\approx$ 1 000 K. It is unlikely, however, that big ($> 0.1\,\mu$m) circumstellar grains develop a clear crystal structure since this requires heating to a temperature of at least 1 200 K, much higher than the stability limit of the silicates.

4.3 Equilibrium chemistry of Mg-Fe ortho-silicates

We now consider the formation of magnesium-iron ortho silicates (olivines) with a mixed composition $\mathrm{Mg}_{2x}\mathrm{Fe}_{2(1-x)}\mathrm{SiO}_4$ with $x \in [0, 1]$ in a chemical equilibrium state. This is considered as a two step process where first pure forsterite $\mathrm{Mg_2SiO_4}$ is formed and then converted into olivine by an exchange reaction with Fe atoms from the gas phase

$$\mathrm{Mg_2SiO_4} + 2(1-x)\mathrm{Fe} \longrightarrow \mathrm{Mg}_{2x}\mathrm{Fe}_{2(1-x)}\mathrm{SiO}_4 + 2(1-x)\mathrm{Mg}\,.$$

We assume that the members of the continuous series of Mg-Fe silicates usually denoted as olivine form a solid solution of forsterite and fayalite. The free enthalpy of formation of one mole of the mixture from x moles of forsterite and $1-x$ moles of fayalite is given by the weighted mean of the free enthalpy of formation of both components and the mixing entropy term

$$\Delta G(\mathrm{Mg}_{2x}\mathrm{Fe}_{2(1-x)}\mathrm{SiO}_4) = x\Delta G(\mathrm{Mg_2SiO_4}) + (1-x)\Delta G(\mathrm{Fe_2SiO_4}) + \Delta G_{\mathrm{mix}} \quad (4.7)$$

where

$$\Delta G_{\mathrm{mix}} = 2RT\,(x\ln x + (1-x)\ln(1-x)) \quad (4.8)$$

(Atkins 1994). In a state of chemical equilibrium between the gas phase and olivine, the partial pressures of Mg and Fe atoms in the gas phase must satisfy the law of mass action

$$p_{\mathrm{Mg}}^{2(1-x)} = p_{\mathrm{Fe}}^{2(1-x)} \cdot \mathrm{e}^{-\Delta G_x/RT} \quad (4.9)$$

where

$$\Delta G_x = \Delta G(\mathrm{Mg}_{2x}\mathrm{Fe}_{2(1-x)}\mathrm{SiO}_4) - \Delta G(\mathrm{Mg_2SiO_4}) + 2(1-x)\,(\Delta G(\mathrm{Mg}) - \Delta G(\mathrm{Fe})) \quad (4.10)$$

is the change of free enthalpy in the conversion of forsterite into olivine. It follows that

$$\frac{p_{\mathrm{Mg}}}{p_{\mathrm{Fe}}} = K_x(T) = \exp\left[-\frac{\Delta G(\mathrm{fay.}) - \Delta G(\mathrm{for.})}{2RT} - \frac{\Delta G_{\mathrm{mix}}}{2(1-x)RT}\right]. \quad (4.11)$$

If f is the fraction of silicon bound in the olivine, the partial pressures of Mg and Fe in the gas phase are $(\epsilon_{\rm Mg} - 2xf\epsilon_{\rm Si})P_{\rm H}$ and $(\epsilon_{\rm Fe} - 2(1-x)f\epsilon_{\rm Si})P_{\rm H}$, respectively. Then

$$\frac{\epsilon_{\rm Mg} - 2xf\epsilon_{\rm Si}}{\epsilon_{\rm Fe} - 2(1-x)f\epsilon_{\rm Si}} = K_x(T, x)\,. \tag{4.12}$$

The degree of condensation f is determined by eqn (4.3) where the term $\epsilon_{\rm Mg} - 2f\epsilon_{\rm Si}$ has to be replaced in the present case by $\epsilon_{\rm Mg} - 2xf\epsilon_{\rm Si}$. Equations (4.12) and (4.3) determine the amount and the composition of the magnesium-iron silicate present in a chemical equilibrium state. We can solve (4.12) for f with the result

$$f = \frac{\epsilon_{\rm Mg} - \epsilon_{\rm Fe}K_x}{2\epsilon_{\rm Si}(x - K_x(1-x))}\,. \tag{4.13}$$

For given x and T eqn (4.13) determines f and then from eqn (4.3) we can determine the total gas pressure corresponding to this state. For fixed x this defines a curve of constant composition x in the P-T-plane. Such curves for selected values of x are shown in the right part of Fig. 10. Obviously, in a rather broad temperature strip below the stability limit of the olivine the chemical equilibrium composition of olivine would be that of nearly pure forsterite. Only at temperatures at least 100 K below the stability limit would substantial amounts of Fe be incorporated into the condensate. Inspection of Fig. 9 or Fig. 10 shows that the iron starts to condense as a separate dust material at similar but slightly higher temperatures as the olivine starts to incorporate substantial amounts of the iron. In constructing Fig. 10 we have assumed that iron is not condensed. The formation of solid iron would reduce the pressure of Fe atoms in the gas phase and this would favour, for given T, an even higher value of x.

Hence, the chemical equilibrium composition of the condensate does not correspond to an iron rich olivine which consumes most of the available Mg and Fe from the gas phase, as it is commonly assumed, but instead it corresponds to a mixture of nearly pure forsterite and metallic iron particles. In Sect. 3.2 we saw that iron nucleation from the gas phase occurs at quite a low temperature. Thus, if iron condenses as a separate solid this is possible at a temperature of about 1 000 K only if it condenses on the surface of already existing grains, which means that small iron nuggets form on the surface of silicate grains. If there exists no process which detaches the iron particles from the surface they will be incorporated as small inclusions into the silicate grains.

4.4 Mg-Fe meta-silicates

At temperatures only slightly less than the stability limit of forsterite the meta-silicate $MgSiO_3$ (enstatite) becomes stable (cf. Fig. 9). It can be shown that the conversion of forsterite into enstatite for instance by the reaction

$$Mg_2SiO_4 + H_2 \longrightarrow MgSiO_3 + Mg + H_2O$$

becomes thermodynamically favourable at a temperature roughly 30 K below the stability limit of the enstatite. Hence it is likely that part of the forsterite formed by condensation from the gas phase is later converted into enstatite. This process will be discussed elsewhere.

4.5 Iron Sulphide (Troilite)

Metallic iron grains may form with the abundant H_2S from the gas phase the quite stable mineral FeS, the troilite. This is observed to be a component of the most primitive meteoritic material and it is also thought to be a component of the interstellar dust (Pollack et al. 1994). The formation of troilite from iron grains occurs according to the reaction

$$\mathrm{Fe_{solid}} \;+\; \mathrm{H_2S} \;\longrightarrow \mathrm{FeS_{solid}} \;+\; \mathrm{H_2}\,.$$

In chemical equilibrium the partial pressures of H_2 and H_2S must satisfy the law of mass action

$$p_{\mathrm{H_2}} = p_{\mathrm{H_2S}} \cdot K_p(T)\,, \tag{4.14}$$

where

$$K_p(T) = \exp\left[-(\Delta G(\mathrm{FeS}) + \Delta G(\mathrm{H_2}) - \Delta G(\mathrm{Fe}) - \Delta G(\mathrm{H_2S}))/RT\right]\,. \tag{4.15}$$

If we assume that the fraction f of the total available iron has reacted to form FeS and if no other abundant sulphur bearing species exist then we have for the partial pressure of H_2S in the gas phase $p_{\mathrm{H_2S}} = (\epsilon_{\mathrm{S}} - f\epsilon_{\mathrm{Fe}})P_{\mathrm{H}}$. From (4.14) it follows

$$f = \frac{1}{\epsilon_{\mathrm{Fe}}}\left(\epsilon_{\mathrm{S}} - \frac{1}{2K_p(T)}\right)\,. \tag{4.16}$$

The maximum fraction of the iron which can be converted into FeS equals the abundance ratio $\epsilon_{\mathrm{S}}/\epsilon_{\mathrm{Fe}} = 0.56$. If the quantity f calculated from equation (4.16) for a certain temperature T takes a value $0 \le f \le 0.56$, then for this temperature the iron metal is partially converted into solid FeS. If there results a value of $f < 0$, then all the iron is present as the free metal and we have to put $f = 0$ in this case. The left part of Fig. 11 shows the result for f for the standard element abundances. The conversion of FeS to Fe extends over a broad temperature region. It starts rather suddenly at a temperature $T \approx 720\,\mathrm{K}$, the conversion of solid Fe into FeS then gradually progresses with decreasing T and it is nearly completed at a temperature of about $500\,\mathrm{K}$, where f approaches the maximum possible value of 0.56. Above the limit temperature defined by $K_p(T) = 1/2\epsilon_{\mathrm{S}}$ the iron always is present as the free metal and no FeS can exist due to reduction of FeS by the abundant hydrogen. Below this temperature the iron would be converted to FeS by reactions with H_2S, but this can convert at most the fraction $f = \epsilon_{\mathrm{S}}/\epsilon_{\mathrm{Fe}}$ of the iron into FeS. If a fraction of the total iron abundance less than this is present as solid iron, the conversion of the metal to FeS would be complete, if the abundance of iron metal exceeds this limit the excess remains as free metal and could be oxidized by water vapour (see Sect. 4.6).

The kinetics of the formation of FeS has been discussed for instance by Fegley and Prinn (1989) and more recently studied in detail in the laboratory by

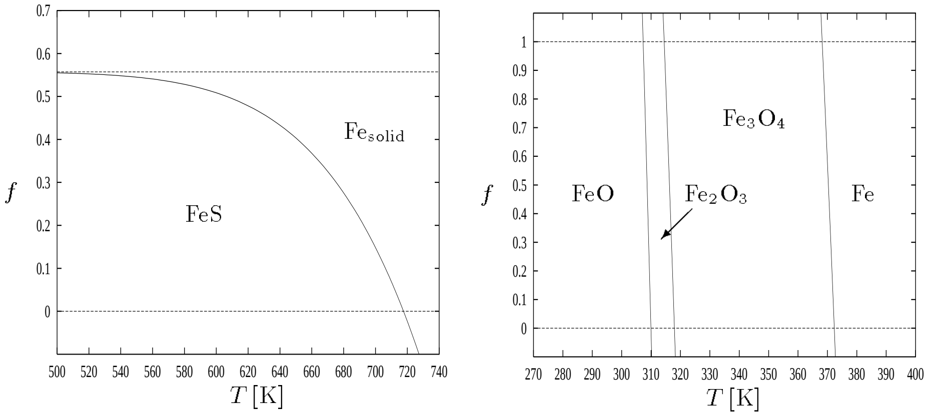

FIG. 11. Left part: Fraction f of the metallic iron which is converted by surface reactions with H_2S into FeS (troilite). Right part: Fraction of the iron converted by surface reactions with H_2O into the indicated iron oxides.

Lauretta et al. (1996). They find a rate coefficient for the formation of FeS from solid Fe of $k_f = 5.6 \cdot \exp(-3360/T)$ in units gram FeS per cm^2, hour, and atm. This holds for the linear kinetics regime where the rate is not controlled by solid diffusion. According to their findings diffusion only becomes important for particle sizes above $10\,\mu$m. This rate may be converted into a radius change of spherical particles of radius a. One obtains

$$\frac{\mathrm{d}a}{\mathrm{d}t} = k_f \cdot \rho_{\mathrm{Tr}}^{-1} = 7.2\,10^{-9}\,\mathrm{e}^{-3360/T}\,p_{\mathrm{H_2S}} \tag{4.17}$$

where $\rho_{\mathrm{Tr}} = 4.7\,\mathrm{g\,cm^{-3}}$ is the density of troilite, the partial pressure of H_2S is now in units dyn cm^{-2}, and a and t are in units of cm and s, respectively. For a particle size of $0.1\,\mu$m and an estimated total pressure $P = 4\,10^{-5}$ dyn cm^{-2} in the circumstellar shell at the temperature of $T = 720\,$K for the onset of FeS formation, we obtain a typical timescale for the conversion of an iron grain of such size into FeS of $t \approx 2\,10^{14}\,$s. Compared with a characteristic timescale for the expansion of the wind of $10^8\,$s in this region this time is much too long for conversion of iron grains into FeS to be possible.

Therefore, though troilite formation would be strongly favoured for chemical reasons it is kinetically inhibited in circumstellar outflows.

4.6 Iron Oxide

Iron oxides are thought to be a possible component of circumstellar dust (e.g. Henning et al. 1995). They may be formed by oxidizing iron grains by water vapour according to the reaction

$$\mathrm{Fe_{solid}} + \mathrm{H_2O} \longrightarrow \mathrm{FeO_{solid}} + \mathrm{H_2}$$

(e.g. Fegley and Prinn 1989). In chemical equilibrium the partial pressures of the molecules have to satisfy the law of mass action

$$p_{\mathrm{H_2}} = p_{\mathrm{H_2O}} \cdot K_p(T)\,, \tag{4.18}$$

where

$$\Delta G = \Delta G(\mathrm{FeO_{solid}}) + \Delta G(\mathrm{H_2}) - \Delta G(\mathrm{Fe_{solid}}) - \Delta G(\mathrm{H_2O})\,. \tag{4.19}$$

If we assume that the fraction f of the totally available iron is oxidized from Fe into FeO and if we admit that some of the oxygen is bound in silicates (g O atoms per Si atom) then we have for the partial pressure of H_2O in the gas phase $p_{\mathrm{H_2O}} = 2(\epsilon_{\mathrm{O}} - \epsilon_{\mathrm{C}} - g\epsilon_{\mathrm{Si}} - f\epsilon_{\mathrm{Fe}})\,P_{\mathrm{H}}$. From (4.18) it follows for f

$$f = \frac{1}{\epsilon_{\mathrm{Fe}}}\left(\epsilon_{\mathrm{O}} - \epsilon_{\mathrm{C}} - g\epsilon_{\mathrm{Si}} - \frac{1}{2K_p(T)}\right)\,. \tag{4.20}$$

If the quantity f calculated from this equation for a certain temperature T takes a value in the interval $0 \le f \le 1$, then for this temperature the iron metal is partially oxidized to FeO. If there results a value of $f > 1$, then the oxidation is complete and we have to put $f = 1$. If there results a value of $f < 0$, then all Fe is present as free iron and we have to put $f = 0$ in this case. The right hand part of Fig. 11 shows the result for f for standard element abundances. It is assumed that silicon atoms have formed solid silicates in which case they have bound four oxygen atoms each ($g = 4$). An inspection of the figure shows that the solid iron metal is oxidized by the water vapour from the gas phase to solid FeO at $T \approx 310\,\mathrm{K}$ and the degree f of oxidation changes from zero to unity within a very narrow temperature interval. Above this temperature, the iron would be present as the free metal and no FeO can exist at such temperatures due to reduction of FeO by the abundant hydrogen. Below this temperature the iron would form FeO due to oxidation by water vapour.

Analogously one determines the limit temperatures for the oxidation or reduction of the two other possible iron oxides. For Fe_2O_3 (hematite) we obtain

$$f = \frac{2}{3\epsilon_{\mathrm{Fe}}}\left(\epsilon_{\mathrm{O}} - \epsilon_{\mathrm{C}} - g\epsilon_{\mathrm{Si}} - \frac{1}{2K_p^{\frac{1}{3}}(T)}\right) \tag{4.21}$$

and for Fe_3O_4 (magnetite)

$$f = \frac{3}{4\epsilon_{\mathrm{Fe}}}\left(\epsilon_{\mathrm{O}} - \epsilon_{\mathrm{C}} - g\epsilon_{\mathrm{Si}} - \frac{1}{2K_p^{\frac{1}{4}}(T)}\right)\,. \tag{4.22}$$

The results for the fraction of the oxidised iron are also shown in the right hand part of Fig. 11. The temperature of formation of Fe_2O_3 is $\approx 330\,\mathrm{K}$ and Fe_3O_4 is formed at $\approx 370\,\mathrm{K}$. Hence above 370 K all iron not bound in silicates, in a chemical equilibrium state would be present as the free metal. Below this temperature it would be oxidized by the water vapour to Fe_3O_4, at temperatures around 315 K this would be converted into Fe_2O_3 and below $\approx 310\,\mathrm{K}$ into FeO.

Free metallic iron cannot exist below $\approx 370\,K$ in chemical equilibrium with the gas phase while the oxides cannot exist above this temperature.

The time required for "rusting" of the iron grains is determined by the reaction kinetics of this process. The activation energy for wustite (FeO) formation in a H_2/H_2O atmosphere, for instance, has been found by Tukdogan et al. (1965) to be $E_a/k = 9\,600\,\mathrm{K}$. In view of this high energy barrier, the low particle density in the wind where rusting becomes chemically favourable, and the findings of the previous Section we can safely conclude that formation of iron oxides, though favourable for chemical reasons, again is kinetically inhibited in the stellar outflow. If iron grains are formed in the condensation zone of the wind, they will not be subject to subsequent chemical modification by surface reactions with species from the gas phase.

5 Concluding remarks

The method and the illustrative applications presented here yield important insights into grain formation in oxygen rich stellar environments, and provide basic information about the condensates to be expected under conditions encountered in circumstellar shells. Of course, these approaches can be considered only as first steps towards a realistic description of inorganic astrophysical grain condensation.

Bibliography

1. Atkins, P.W. (1994). *Physical Chemistry*, 5th Ed., Oxford University Press, Oxford.
2. Anders, E. and Grevesse, N. (1989). *Geochimica et Cosmochimica Acta*, **53**, 197.
3. Ashworth, J.R., Mallinson, L.G., Hutchinson, R. and Biggar, G.M. (1984). *Nature*, **308**, 259.
4. Catti, M. (1986). in *Chemistry and Physics of Terrestrial Planets*, S.K. Saxena Ed., Springer, New York, 224.
5. Dekker A.J. (1963). *Solid State Physics*. Macmillan, London.
6. Deguchi, S. (1980). *Astrophysical J.*, **236**, 567.
7. Donn, B. and Nuth, J.A. (1985). *Astrophysical J.*, **288**, 187.
8. Donn, B., Wickramasinghe, N.C., Hudson, J.P. and Stecher, T.P. (1968). *Astrophysical J.*, **153**, 451.
9. Dorschner, J. and Henning, T. (1995). *Astronomy & Astrophysics Rev.*, **6**, 271.
10. Draine, B.T. (1979). *Astrophys. Space Sci.*, **65**, 311.
11. Draine, B.T. and Salpeter, E.E. (1977). *J. Chem. Phys.*, **67**, 2230.
12. Duschl, W.J., Gail, H.-P. and Tscharnuter, W.M. (1996). *Astronomy & Astrophysics*, **312**, 624.
13. Evans, R.C. (1966). *An Introduction to Crystal Chemistry*, 2nd Ed., Cam-

bridge University Press, Cambridge.

14. Feder, J., Russel, K.C., Lothe, J. and Pound, G.M. (1966). *Adv. Phys.*, **15**, 111.
15. Fegley Jr., B. and Prinn, R.G. (1989). in *The Formation and Evolution of Planetary Systems*, H.A. Weaver and L. Danly Eds., Cambridge University Press, Cambridge, 171.
16. Gail, H.-P. and Sedlmayr, E. (1984). *Astronomy & Astrophysics*, **132**, 163.
17. Gail, H.-P. and Sedlmayr, E. (1986). *Astronomy & Astrophysics*, **166**, 225.
18. Gail, H.-P. and Sedlmayr, E. (1987). in *Physical Processes in Interstellar Clouds*, G. Morfill and M. Scholer Eds., Reidel, Dordrecht, 275.
19. Gail, H.-P. and Sedlmayr, E. (1988). *Astronomy & Astrophysics*, **206**, 153.
20. Gail, H.-P., Keller, R. and Sedlmayr, E. (1984). *Astronomy & Astrophysics*, **133**, 320.
21. Goebel, J.H., Bregman, J.D. and Witteborn, F.C. (1994). *Astrophysical J.*, **430**, 317.
22. Grevesse, N. and Noels, A. (1993). in *Origin and Evolution of the Elements*, N. Prantzos, E. Vangioni-Flam and M. Cassé Eds., Cambridge University Press, Cambridge, 14.
23. Habing, H.J. (1996). *Astronomy & Astrophysics Rev.* **7**, 97.
24. Henning, Th., Begemann, B., Mutschke, H. and Dorschner, J. (1995). *Astronomy & Astrophysics Suppl.*, **112**, 143.
25. Iben Jr., I. (1991). *Astrophysical J. Suppl.*, **76**, 55.
26. John, M. (1995). Bildung von Eisen-Clustern in kühlen Sternwinden. Diploma thesis, Technical University Berlin.
27. John, M. and Sedlmayr, E. (1998). Formation of iron clusters in cool stellar winds (in preparation).
28. Köhler, T.M., Gail, H.-P. and Sedlmayr, E. (1997). *Astronomy & Astrophysics*, **320**, 553.
29. Kozasa, T. and Hasegawa, H. (1987). *Prog. Theor. Phys.*, **77**(6), 1402.
30. Kuskov, O.L. and Galimzyanov, R.F. (1986). in *Chemistry and Physics of Terrestrial Planets*, S.K. Saxena Ed., Springer, New York, 310.
31. Lauretta, D.S., Kremser, D.T. and Fegley Jr., B. (1996). *Icarus*, **122**, 288.
32. Lenzuni, P., Gail, H.-P., Henning, Th. (1995). *Astrophysical J.*, **447**, 848.
33. Lian, L., Su, C.-X. and Armentrout, P. (1992). *J. Chem. Phys.*, **97**(6), 4072.
34. Lide, D.R. (1995). *Handbook of Chemistry and Physics*, 76th Edn., CRC Press, Boca Raton.
35. Loup, C., Forveille, T., Omont, A. and Paul, J.F. (1993). *Astronomy & Astrophysics Suppl.*, **99**, 291.
36. Martin, T.P. (1983). *Phys. Rep.*, **95**, 167.
37. Nuth, J.A. and Donn, B. (1981). *Astrophysical J.*, **247**, 925.

38. Nuth, J.A. and Donn, B. (1982a). *Astrophysical J.*, **257**, L103.
39. Nuth, J.A. and Donn, B. (1982b). *J. Chem. Phys.*, **77**(5), 2639.
40. Nuth III, J.A. and Hecht, J.H. (1990). *Astrophys. Space Sci.*, **163**, 79.
41. Nuth III. J.A., Donn, B. and Nelson, R. (1986). *Astrophysical J.*, **310**, L83.
42. Pollack, J.B., Hollenbach, D., Beckwith, S., Simonelli, D.P., Roush, T. and Fong, W. (1994). *Astrophysical J.*, **412**, 615.
43. Rowan-Robinson, M. and Harris, S. (1983). *Monthly Notices Roy. Astr. Soc.*, **202**, 767.
44. Salpeter, E.E. (1974). *Astrophysical J.*, **193**, 579.
45. Sedlmayr, E. and Dominik, C. (1995). *Space Science Rev.*, **73**, 211.
46. Sharp, C.M. and Hübner, W.F. (1990). *Astrophysical J. Suppl*, **72**, 417.
47. Shim, I. and Gingerich, K. (1982). *J. Chem. Phys.*, **77**, 2490.
48. Smith, V.V. and Lambert, L.L. (1990). *Astrophysical J. Suppl.*, **72**, 387.
49. Sylvester, R.J., Barlow, M.J. and Skinner, C.J. (1994). *Monthly Notices Roy. Astr. Soc.*, **266**, 640.
50. Turkdogan, E.T., McKewan, W.M. and Zwell, L. (1965). *J. Phys. Chem.*, **69**, 327.
51. Waters, L.B.E.M. and 36 others (1996). *Astronomy & Astrophysics*, **315**, L361.
52. Yamamoto, T. and Hasegawa, H. (1977). *Progr. Theor. Phys.*, **58**, 816.